

An Experimental Demonstration of 160-Gbit/s PAM-4 Using a Silicon Micro-Ring Modulator

Yeyu Tong^{ID}, Zhouyi Hu^{ID}, Xinru Wu^{ID}, Songtao Liu^{ID}, Lin Chang, Andrew Netherton, Chun-Kit Chan^{ID}, John E. Bowers^{ID}, and Hon Ki Tsang^{ID}

Abstract—Silicon photonics has been regarded as a promising technology for future small-footprint, low-cost and low-power 400-Gbit/s datacenter interconnects (DCIs). In this work, for the first time, we report an experimental demonstration of a single-wavelength, single-polarization 160-Gbit/s four-level pulse-amplitude modulation (PAM-4) employing a single integrated silicon carrier-depletion micro-ring modulator (MRM). The measured bit-error rates (BERs) for the back-to-back (BTB) and after 1-km standard single-mode fiber (SSMF) transmission are $1.36\text{E-}3$ and $2.12\text{E-}3$, respectively, all below the **hard-decision forward error correction (HD-FEC) coding limit with 7% overhead**. A data rate of up to 170 Gbit/s with a BER lower than the HD-FEC limit is demonstrated for the BTB transmission.

Index Terms—Datacenter interconnects, silicon photonics, micro-ring modulator, short-reach communication.

I. INTRODUCTION

SILICON photonics has received considerable industry interest for 100-Gbit/s and future 400-Gbit/s high-capacity optical datacenter interconnects (DCIs) applications, due to the unique benefits of the complementary metal-oxide-semiconductor (CMOS) compatibility, a large-scale integration ability, and a low cost for large-volume manufacturing [1]. Realizing a $4 \times > 100$ -Gbit/s data rate transmission by integrated silicon photonic transceivers is thus highly desired in accordance with the IEEE 400G Ethernet standard. It imposes a stringent requirement on the high-bandwidth integrated optoelectronic devices such as the optical modulators.

High-speed optical modulators on the silicon photonics platform relying on the free-carrier plasma dispersion effect include the Mach-Zehnder modulators [2]–[5] and the micro-ring modulators (MRMs) [5]–[7]. The recently reported germanium-on-silicon electro-absorption modulators relying

on the Franz-Keldysh effect also manifest attractive features for applications in the short-reach optical DCIs [8]–[10].

Silicon MRMs manifest various distinct advantages such as a compact device footprint with a diameter of about $10\text{ }\mu\text{m}$ [11]. A low driving voltage and a small device capacitance can be enabled by confining the light in a tiny ring cavity. The modulation speed is thus significantly improved with less limitations induced by the resistance-capacitance (RC) time. A low energy consumption of as small as 1 fJ/bit has been experimentally demonstrated [12]. Thanks to the multiple functionalities of the micro-ring, attractive wavelength-division multiplexing (WDM) transmitters can be realized by cascading the MRM array with the multi-wavelength sources, without employing additional WDM multiplexers [13]–[15].

Silicon MRMs have been widely investigated over the past years. The frequency response of the MRM is determined by the cavity photon lifetime and the p-n junction RC response. The modulator bandwidth limit can be improved by increasing the p-n junction doping with a reduced quality (Q) factor. However, the extinction ratio also decreases with additional insertion loss and capacitance. An intrinsic trade-off thus exists between the modulator bandwidth and the modulator optical loss [5]. Up to a 50-GHz electro-optical (EO) bandwidth has been demonstrated [5], [6]. Advanced modulation formats using silicon MRMs can be realized such as the four-level pulse-amplitude modulation (PAM-4) [6], orthogonal frequency-division multiplexing (OFDM) [16] and quadrature amplitude modulation (QAM) [17], [18].

For > 100 -Gbit/s single-lane-rate intensity modulation and direct-detection (IM/DD) short-reach communications systems, advanced digital signal processing (DSP) techniques can also be applied to enable the ultimate potentials of the integrated silicon photonic components. Despite concerns on the increased power consumption and cost, with a growing bandwidth demand, DSP is considered as a necessary enabler of a higher data rate and higher-order modulation formats for future short-reach communications [19]. By using a ten-channel MRM array with discrete multi-tone (DMT) modulation, researchers have achieved an aggregated data rate of 0.88 Tbit/s [15]. A single-lane rate of 128-Gbit/s PAM-4 experiment using a 50-GHz MRM was also demonstrated [6].

In this Letter, a carrier-depletion silicon MRM with a high modulation bandwidth is driven by a high-speed digital-to-analog converter (DAC) with DSP techniques.

Manuscript received September 9, 2019; revised December 12, 2019; accepted December 13, 2019. Date of publication December 16, 2019; date of current version January 15, 2020. This work was supported in part by the Hong Kong Research Grants Council General Research Fund under Grant 14212816 and in part by the Advanced Research Projects Agency-Energy (ARPA-E) under the ENLITENED Program under Grant DE-AR0000843. (Corresponding author: Hon Ki Tsang.)

Y. Tong, X. Wu, and H. K. Tsang are with the Department of Electronic Engineering, The Chinese University of Hong Kong, Hong Kong (e-mail: hktsang@ee.cuhk.edu.hk).

Z. Hu and C.-K. Chan are with the Department of Information Engineering, The Chinese University of Hong Kong, Hong Kong.

S. Liu, L. Chang, A. Netherton, and J. E. Bowers are with the Department of Electrical and Computer Engineering, University of California at Santa Barbara, Santa Barbara, CA 93106 USA.

Color versions of one or more of the figures in this letter are available online at <http://ieeexplore.ieee.org>.

Digital Object Identifier 10.1109/LPT.2019.2960238

1041-1135 © 2019 IEEE. Personal use is permitted, but republication/redistribution requires IEEE permission.

See http://www.ieee.org/publications_standards/publications/rights/index.html for more information.

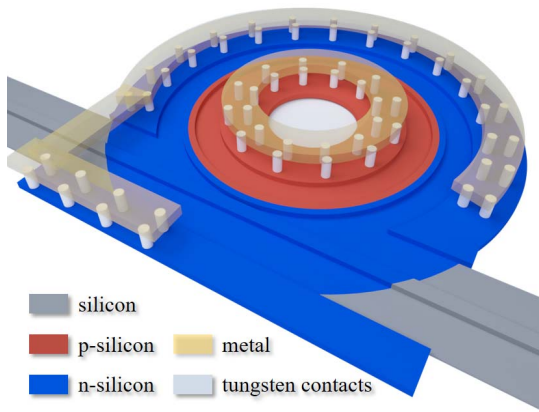


Fig. 1. Schematic structure of the integrated silicon MRM.

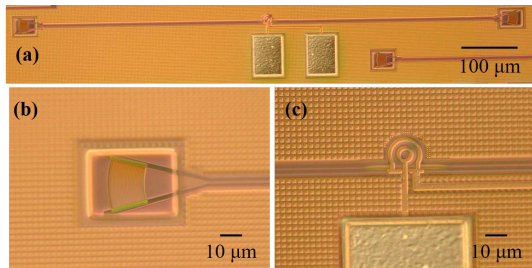


Fig. 2. (a) Optical microscopic image of the silicon photonic chip. (b) Zoom-in view of the grating coupler. (c) Zoom-in view of the silicon MRM.

We report the first, to the best of our knowledge, experimental demonstration of a single-wavelength, single-polarization 160-Gbit/s PAM-4 transmission using a single integrated silicon MRM. The obtained bit-error rate (BER) performance after 1-km standard single-mode fiber (SSMF) transmission is well below the hard-decision forward error correction (HD-FEC) coding limit with 7% overhead. Data rate of up to 170-Gbit/s PAM-4 is also reported for the back-to-back (BTB) IM/DD system with a BER under the HD-FEC limit.

II. DEVICE CHARACTERIZATION

The silicon MRM is fabricated at the IMEC in a multi-project wafer run under the platform of ISIPP50G [5]. The silicon-on-insulator (SOI) wafer has a 220-nm silicon layer and a 2-μm buried-oxide layer. A schematic structure of the MRM is shown in Fig. 1. The silicon rib waveguide has a width of 500 nm with a 60-nm-thick slab. The ring cavity has a diameter of 10 μm with a ring-bus gap spacing of 150 nm. A symmetric lateral p-n doping is applied on the resonator. The MRM is based on the carrier-depletion configuration for high-speed modulation. The highly doped silicon contacts the metal layer via tungsten. Fig. 2 are the optical microscopic images of the photonic chip showing the MRM, the bond pads and the grating couplers via a 10° off-vertical coupling. The in-and-out loss of the grating coupler is about 5.5 dB interfacing with a SSMF with a mode-field diameter of 10.4 μm.

Fig. 3(a) shows the transmission spectra of the MRM under a reverse-bias voltage from 0 V to −5 V. The resonant

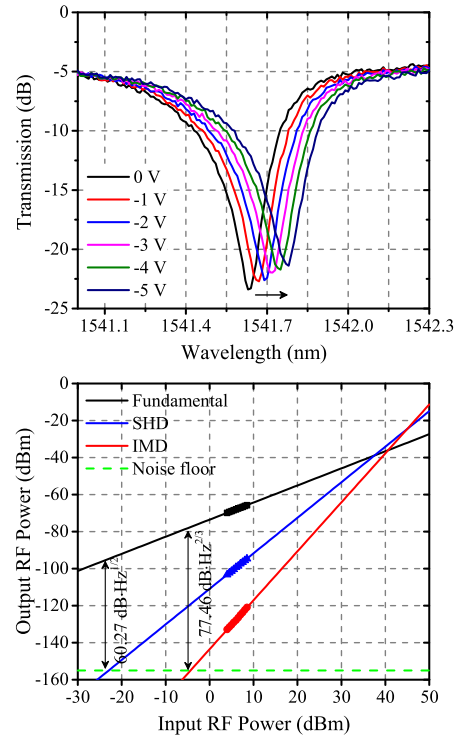


Fig. 3. (a) Transmission spectra of the MRM under a reverse-bias voltage from 0 V to −5 V. (b) Spurious-free dynamic range of the MRM characterized at 10 GHz with a resolution bandwidth of 10 Hz. The noise floor is −155 dBm.

wavelength is red-shifted with increasing the reverse-bias, as the refractive index increases upon depleting carriers while the depletion region is widened. The tuning efficiency of the MRM is about 33 pm/V. The MRM has a free spectral range (FSR) of 19.5 nm and a Q factor of about 3000. To evaluate the modulator linearity for advanced modulation formats, the spurious-free dynamic range (SFDR) of the MRM is measured with results shown in Fig. 3(b). The second-order harmonic distortion (SHD) and the third-order intermodulation distortion (IMD) are characterized at a frequency of 10 GHz. The resolution bandwidth of the radio-frequency (RF) spectrum analyzer (Rohde & Schwarz FSW43) is set at 10 Hz. After curve-fitting of the 8 measured data points, the obtained $SFDR_{SHD}$ and $SFDR_{IMD}$ for the silicon MRM are $60.27 \text{ dB} \cdot \text{Hz}^{1/2}$ and $77.46 \text{ dB} \cdot \text{Hz}^{2/3}$, respectively. The limited linearity of the MRM also introduces impairments in the short-reach system, which can be compensated by DSP, but will not be discussed in this work. The modulator frequency response is measured at −0.12 nm offset from the resonance transmission dip by a 67-GHz network analyzer and a light-wave component analyzer (Agilent Technologies, N4373C and E8361A) as shown in Fig. 4. The p-n junction capacitance reduces with a larger reverse-bias voltage, and the 3-dB EO bandwidth of the MRM is about 36 GHz and 47 GHz when biased at 0 V and −2.5 V, respectively.

III. EXPERIMENTAL SETUP AND DIGITAL SIGNAL PROCESSING

The experimental setup and the DSP flow for the 160-Gbit/s IM/DD system using the integrated silicon MRM is shown

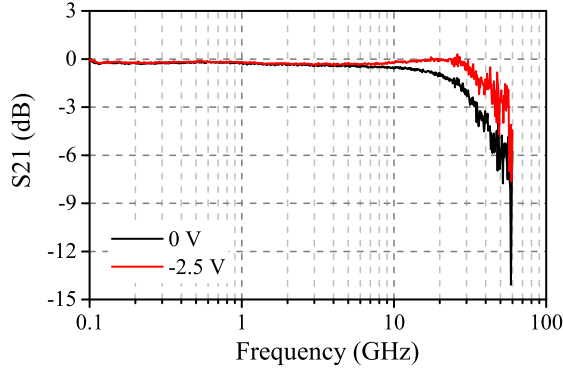


Fig. 4. Frequency response of the MRM at the bias voltage of 0 V and -2.5 V at a detuning of -0.12 nm.

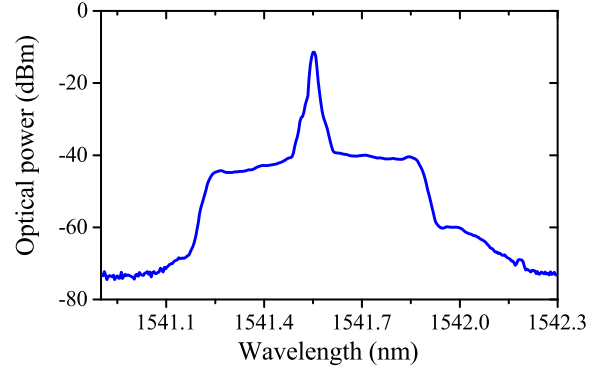


Fig. 6. Optical spectrum measured with a resolution bandwidth of 0.016 nm for 80-Gbaud/s PAM-4 signals generated by the silicon MRM.

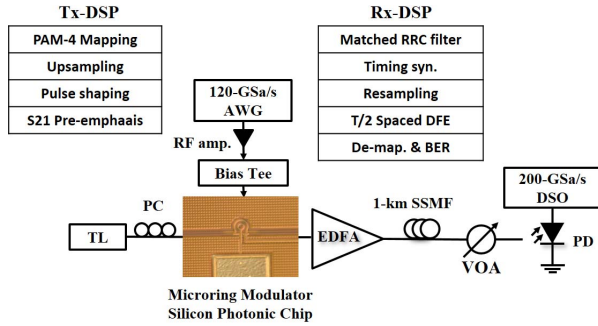


Fig. 5. Experimental setup and digital signal processing flow for the >100-Gb/s intensity modulation and direct detection (IM/DD) system using the silicon MRM, including the arbitrary waveform generator (AWG), RF amplifier (RF amp.), bias tee, tunable laser (TL), polarization controller (PC), erbium doped fiber amplifier (EDFA), standard single-mode fiber (SSMF), variable optical attenuator (VOA) and digital storage oscilloscope (DSO).

in Fig. 5. An output **optical power of 6 dBm** is launched into the silicon photonic chip via a wavelength-tunable laser at **1541.57 nm**. The MRM is reverse-biased at -2.5 V using a 65-GHz bias tee (Anritsu V252). The arbitrary waveform generator (AWG, Keysight 8194A) has a sampling rate of 120 GSa/s. The electrical signal is amplified to about 2.4-V peak-to-peak voltage by an RF amplifier (SHF S807C) with a 3-dB bandwidth of 55 GHz. The optical signal from the output grating coupler is boosted by an erbium-doped fiber amplifier (EDFA, Amonics AEDFA-PA-30) before transmission. A 50-GHz p-i-n photodiode (PD, U2T 2120RA) is used at the receiver side without a trans-impedance amplifier (TIA). The received optical power is controlled by a variable **optical attenuator** (VOA). The digital storage oscilloscope (DSO, Tektronix DPO 70000SX ATI) has a sampling rate of 200 GSa/s. The received signal is recovered by the offline processing. At the transmitter side, the 80-Gbaud/s PAM-4 signal is up-sampled by a factor of 1.5 (120/80). A root-raised-cosine (RRC) filter with a roll-off factor of 0.12 is implemented for the Nyquist pulse shaping. The up-sampled signal is pre-emphasised by using an inverted linear filter based on the channel frequency response measured with a probe signal. At the receiver side, a matched RRC filter is performed to mitigate the effects of white noise. The received signal is re-sampled to two samples per symbol. The feed-forward

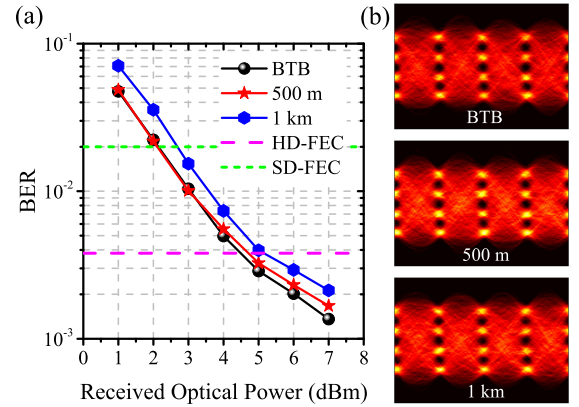


Fig. 7. (a) BER performance of the MRM-based 160-Gbit/s PAM-4 IM/DD system, for the BTB, after 500-m and 1-km SSMF transmission. SD-FEC: soft-decision forward error correction, HD-FEC: hard-decision forward error correction. (b) Eye diagrams of PAM-4 signals with different transmission lengths at 7-dBm received optical power.

and feedback filters have 33 and 9 taps, respectively for the decision-feedback equalizer (DFE) before error counting.

IV. EXPERIMENTAL RESULTS

Fig. 6 shows the measured optical spectrum of the 80-Gbaud PAM-4 signal by an optical spectrum analyzer (OSA) with a resolution bandwidth of 0.016 nm. The signal effective bandwidth is reduced to 44.8 GHz due to the pulse shaping with a roll-off factor of 0.12 applied at the transmitter side.

Fig. 7(a) presents the BER performance of the 160-Gbit/s PAM-4 signal against the received optical power in the BTB, after 500-meter and 1-km SSMF transmission. The obtained optimum BERs are $1.36\text{E-}3$, $1.67\text{E-}3$ and $2.12\text{E-}3$, respectively at 7-dBm received optical power. All are below the hard-decision forward error correction (HD-FEC) coding limit with 7% overhead. The required received optical powers are about 5 dBm at the HD-FEC threshold due to the limited sensitivity of the PD without a TIA. Clearly open eye diagrams of the received PAM-4 signals with different transmission lengths are shown in Fig. 7(b). The BER performance against the data rate of the MRM-based PAM-4 IM/DD BTB system is shown in Fig. 8. Up to a 170-Gbit/s data rate is achieved for

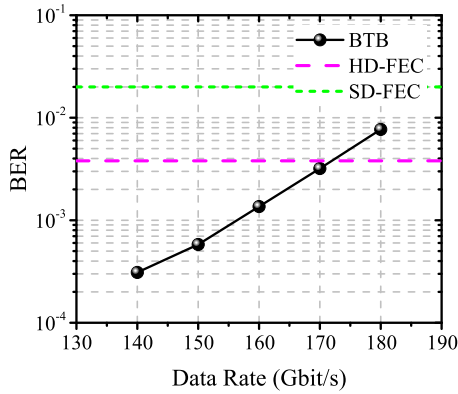


Fig. 8. BER performance against the data rate of the MRM-based PAM-4 IM/DD BTB system at a received optical power of 7 dBm.

the BTB system with a BER of $3.2\text{E}-3$, which is also lower than the HD-FEC limit at $3.8\text{E}-3$.

V. CONCLUSION

In this work, we demonstrated an MRM-based PAM-4 IM/DD short-reach communications system. A record data rate of 160 Gbit/s using a single silicon MRM has been demonstrated with a transmission over 1-km SSMF. The obtained BER performance was below the HD-FEC limit. A data rate of up to 170 Gbit/s for the BTB system was obtained. Our demonstration validates the state-of-art result achieved using a single silicon MRM and shows its potentials for the next-generation 400-Gbit/s DCIs and beyond. Potential improvement on the silicon MRMs with a better modulation efficiency and a reduced junction capacitance can be realized by optimizing the doping design [6], [20], [21]. Additional improvement of link performance may be achieved by further optimization of the receiver equalizer and applying the non-linear pre-distortion technique [22]. An extended transmission length can be realized in the future by moving to the O-band with less CD-induced penalty [6], [7], or applying the coherent techniques with digital CD equalization [17], [18].

ACKNOWLEDGEMENT

The authors acknowledge IMEC for the device fabrication. The authors also thank G. M. Brodnik and D. J. Blumenthal for discussions and assistance with the arbitrary waveform generator.

REFERENCES

- [1] R. Jones *et al.*, "Heterogeneously integrated InP/silicon photonics: Fabricating fully functional transceivers," *IEEE Nanotechnol. Mag.*, vol. 13, no. 2, pp. 17–26, Apr. 2019.
- [2] P. Dong, L. Chen, and Y.-K. Chen, "High-speed low-voltage single-drive push-pull silicon mach-zehnder modulators," *Opt. Express*, vol. 20, no. 6, pp. 6163–6169, 2012.

- [3] F. Zhang *et al.*, "Up to single lane 200G optical interconnects with silicon photonic modulator," in *Proc. Opt. Fiber Commun. Conf. Exhib. (OFC)*, 2019, pp. 1–3.
- [4] A. Samani *et al.*, "Experimental parametric study of 128 Gb/s PAM-4 transmission system using a multi-electrode silicon photonic Mach Zehnder modulator," *Opt. Express*, vol. 25, no. 12, pp. 13252–13262, 2017.
- [5] M. Pantouvaki *et al.*, "Active components for 50 Gb/s NRZ-OOK optical interconnects in a silicon photonics platform," *J. Lightw. Technol.*, vol. 35, no. 4, pp. 631–638, Feb. 15, 2017.
- [6] J. Sun, R. Kumar, M. Sakib, J. B. Driscoll, H. Jayatilaka, and H. Rong, "A 128 Gb/s PAM4 silicon microring modulator with integrated thermo-optic resonance tuning," *J. Lightw. Technol.*, vol. 37, no. 1, pp. 110–115, Jan. 1, 2018.
- [7] Y. Ban *et al.*, "Low-voltage 60 Gb/s NRZ and 100 Gb/s PAM4 O-band silicon ring modulator," in *Proc. IEEE Opt. Interconnects Conf. (OI)*, Apr. 2019, pp. 1–2.
- [8] Y. Tong *et al.*, "112-Gb/s PAM-4 using integrated germanium on silicon franz-Keldysh modulator," in *CLEO: Science and Innovations*. Washington, DC, USA: Optical Society of America, 2018, Paper SM4B-4.
- [9] J. Verbist *et al.*, "DAC-less and DSP-free 112 Gb/s PAM-4 transmitter using two parallel electroabsorption modulators," *J. Lightw. Technol.*, vol. 36, no. 5, pp. 1281–1286, Mar. 1, 2018.
- [10] Y. Tong *et al.*, "Negative frequency-chirped 112-Gb/s PAM-4 using an integrated germanium franz-Keldysh modulator," *IEEE Photon. Technol. Lett.*, vol. 30, no. 16, pp. 1443–1446, Aug. 15, 2018.
- [11] Q. Xu, B. Schmidt, S. Pradhan, and M. Lipson, "Micrometre-scale silicon electro-optic modulator," *Nature*, vol. 435, no. 7040, p. 325, 2005.
- [12] R. Dubé-Demers, S. LaRochelle, and W. Shi, "Ultrafast pulse-amplitude modulation with a femtojoule silicon photonic modulator," *Optica*, vol. 3, no. 6, pp. 622–627, 2016.
- [13] Q. Xu, B. Schmidt, J. Shakya, and M. Lipson, "Cascaded silicon micro-ring modulators for WDM optical interconnection," *Opt. Express*, vol. 14, no. 20, pp. 9431–9436, 2006.
- [14] S. Liu *et al.*, "High-channel-count 20 GHz passively mode-locked quantum dot laser directly grown on Si with 4.1 Tbit/s transmission capacity," *Optica*, vol. 6, no. 2, pp. 128–134, 2018.
- [15] P. Dong, J. Lee, K. Kim, Y.-K. Chen, and C. Gui, "Ten-channel discrete multi-tone modulation using silicon microring modulator array," in *Proc. Opt. Fiber Commun. Conf.*, 2016, Paper W4J-4.
- [16] X. Wu, C. Huang, K. Xu, C. Shu, and H. K. Tsang, "128-Gb/s line rate OFDM signal modulation using an integrated silicon microring modulator," *IEEE Photon. Technol. Lett.*, vol. 28, no. 19, pp. 2058–2061, Oct. 1, 2016.
- [17] P. Dong, C. Xie, L. Chen, N. K. Fontaine, and Y.-K. Chen, "Experimental demonstration of microring quadrature phase-shift keying modulators," *Opt. Lett.*, vol. 37, no. 7, pp. 1178–1180, 2012.
- [18] Y. Tong, Q. Zhang, X. Wu, C. Shu, and H. K. Tsang, "112 Gb/s 16-QAM OFDM for 80-km datacenter interconnects using silicon photonic integrated circuits and Kramers-Kronig detection," *J. Lightw. Technol.*, vol. 37, no. 14, pp. 3532–3538, Jul. 15, 2019.
- [19] K. Zhong, X. Zhou, J. Huo, C. Yu, C. Lu, and A. P. T. Lau, "Digital signal processing for short-reach optical communications: A review of current technologies and future trends," *J. Lightw. Technol.*, vol. 36, no. 2, pp. 377–400, Jan. 15, 2018.
- [20] M. Pantouvaki *et al.*, "Comparison of silicon ring modulators with interdigitated and lateral PN junctions," *IEEE J. Sel. Topics Quantum Electron.*, vol. 19, no. 2, Mar./Apr. 2012, Art. no. 7900308.
- [21] X. Xiao *et al.*, "44-Gb/s silicon microring modulators based on zigzag PN junctions," *IEEE Photon. Technol. Lett.*, vol. 24, no. 19, pp. 1712–1714, Oct. 1, 2012.
- [22] H. Li *et al.*, "A 112 Gb/s PAM4 transmitter with silicon photonics microring modulator and CMOS driver," in *Proc. Opt. Fiber Commun. Conf. Exhib. (OFC)*, 2019, pp. 1–3.